

Review Results on Wing-Body Interference

Vladimir Frolov^{1,a}

¹Samara National Research University, Design and Aircraft Construction Department, 443086 Samara, Russia

Abstract. The paper presents an overview of results for wing-body interference, obtained by the author for varied wing-body combinations. The lift-curve slopes of the wing-body combinations are considered. In this paper a discrete vortices method (DVM) and 2D potential model for cross-flow around fuselage are used. The circular and elliptical cross-sections of the fuselage and flat wings of various forms are considered. Calculations showed that the value of the lift-curve slopes of the wing-body combinations may exceed the same value for an isolated wing. This result confirms an experimental data obtained by other authors earlier. Within a framework of the used mathematical models the investigations to optimize the wing-body combination were carried. The present results of the optimization problem for the wing-body combination allowed to select the optimal geometric characteristics for configuration to maximize the values of the lift-curve slopes of the wing-body combination. It was revealed that maximums of the lift-curve slopes for the optimal mid-wing configuration with elliptical cross-section body had a sufficiently large relative width of the body (more than 30% of the span wing).

1 Introduction

An analysis of a lift for the wing-body combinations nowadays still plays an important role in a theoretical research of an aerodynamic and a preliminary design of modern aircraft.

Aircraft designers have been interested in problems of the aerodynamic wing-fuselage combination in aviation and missile technology since the aircraft occurrence. Initially, investigations were focused on the experimental study of the specific wing-body combinations [1-6]. The next years, there were theoretical papers, in which first mathematical models of the wing-fuselage interference were offered. Exact solution even for the linearized problem of the ideal incompressible flow around arbitrary shape wings in the presence of the fuselage is a difficult task, since it is necessary to solve the three-dimensional Laplace equation for the velocity potential which satisfies the boundary conditions on the surface of the combination and at infinity. The first exact solution of this problem was obtained in Golubinsky's paper [7]. The first mathematical models were based on using disposition of vortices inside the fuselage [8], on an approximate representation of integral equations [9], on the thin body theory [10-21], on the strips method [14, 15, 22] and on the calculation of the lift by the found in Trefftz's plane using velocity potential [23-26] or stream function [27]. The distribution of lift along the wing span can be obtained using methods based on the consideration of the velocity potential in the Trefftz's plane [22-26, 28-30]. It is possible to note an important result that was first obtained theoretically by Multhopp [22] and was

confirmed experimentally by Jacobs and Ward [1]. This result is that the lift-curve slope of the wing-fuselage combination at a certain relative value diameter of the fuselage $\bar{D} = d_f/b$ (where d_f is the diameter of the fuselage; b is the wing span) exceeds the same value for the isolated wing of the same geometry which is used in the wing-body configuration. Here are some examples that confirm this fact. It was obtained that for the scheme mid-wing monoplane with cylindrical fuselage $\bar{D} = 0.14$ and trapezoidal wing with aspect ratio $AR = 4.83$ and taper ratio $\lambda = 2,38$ the value lift-curve slope of the wing-fuselage combination $C_{L_{\alpha, W.B}}$ exceeds the same value $\bar{C}_{L_{\alpha, W}}$ for the isolated wing of the same geometry which is used in the wing-body configuration by approximately 5% (4.75% – an experiment; 4.92% – theory) [22]. It was obtained also that for the wing-body combination №13 in the experimental Jacobs's and Ward's paper [1] relative increase in the lift-curve slope of the wing-fuselage combination was a slightly greater ($\approx 6.49\%$) compared with the isolated wing of the same geometry. In Korner's book [6] you can read that the lift-curve slope of the wing-fuselage combination is some 5% higher than that of the wing alone. Excess value of the lift-curve slope of the wing-fuselage combination above the same magnitude for the isolated wing of the same geometry is also noted in the theoretical papers [31, 32]. In paper [32] on the basis of approximate method for the scheme mid-wing monoplane ($AR = 16; \lambda = 1; \bar{D} = D_f/b \approx 0,25$) was received an

^a Corresponding author: frolov_va_ssau@mail.ru

increase of the lift-curve slope of the wing-fuselage combination compared with the isolated wing with the same geometry approximately 19%. Theoretical calculations the lift-curve slope of the wing-fuselage combination are devoted also book [33] and papers [34-36]. This review is by no means covers all papers on the interference of the wing and fuselage. Author's book [37] contains more a detailed bibliography on the problems of the lift of the wing-body combination.

The main purpose of this paper is to demonstrate conformity of computational results obtained by the author with the known experimental and theoretical results of other authors, as well as to give results of solving optimization problems for lift wing-body configurations.

2 Mathematical model of the wing-body interference

Mathematical model of the wing-body interference included two methods: 1) a discrete vortices method (DVM) and 2) 2D potential model for cross-flow around fuselage [37].

The original three-dimensional problem (Fig. 1) is divided into two: two-dimensional problem of the flow around cross section of the fuselage (Fig. 2) and three-dimensional problem for the isolated wing. The method consists in the fact that in the 2D problem of flow cross-section of the fuselage is added a pair of discrete point vortices. The vortices are the consequence arising lift on the wing. According to Zhukovsky's theory about lift of the wing, any lifting surface can be replaced by an equivalent Π -shaped vortex, its free vortices at low angles of attack lie in the plane of the wing and extends to infinity. In this model is offered that each console part of the wing replaced by a single Π -shaped vortex lying in the plane of the wing. In Fig. 1, the Π -shaped vortex shown in the left wing console. The intensity and the coordinate of the free vortex can find from the constraint equations after will be calculated lift isolated wing by DVM.

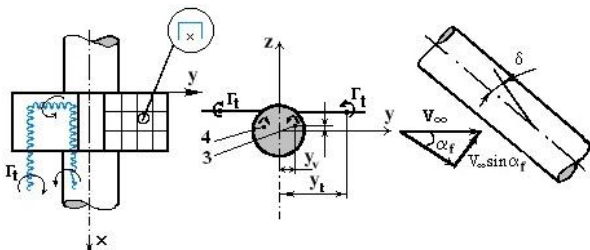


Figure 1. About model wing-body interference

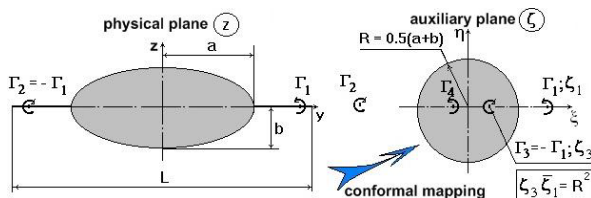


Figure 2. About model potential flow around elliptical cross-section of fuselage in present pair vortices

In order to satisfy the boundary conditions of impermeability on the surface of the body cross section for canonical body vortices can use inversion method (Fig. 2) and for the arbitrary two-dimensional cross section can use the panel method. Fig. 3 shows an example of the potential flow solutions for flow around elliptical cross-section of fuselage in present pair vortices.

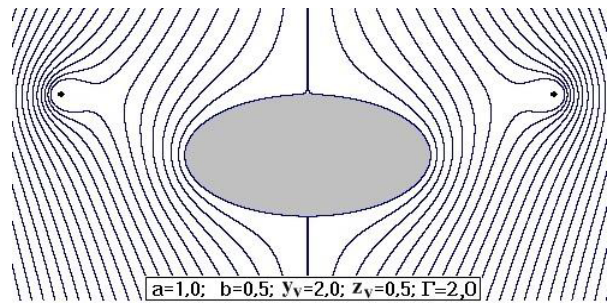


Figure 3. Example potential flow around elliptical cross-section of fuselage in present pair vortices

In this formulation, the problem is reduced to solving the following system of algebraic linear equations

$$\sum_{i=1}^L \Gamma_i (\mathbf{A}_{ij} \cdot \mathbf{n}_j) = -(\mathbf{F}_j \cdot \mathbf{n}_j), \quad j = 1, \dots, L, \quad (1)$$

where Γ_i is a column vector composed of unknown intensities of attached vortices; \mathbf{n}_j is the unit normal vector to the j -th control point on the wing surface; \mathbf{A}_{ij} is the matrix of the aerodynamic influence or the matrix of the induced velocities at the control points of the wing surface from all system of horseshoe vortices (left and right consoles for the isolated wing); \mathbf{F}_j is column vector of the velocity induced in the j -th the control point on the wing surface by incoming flow and the flow from the cross section of the fuselage that includes either inversion of the vortices or sources and sinks providing satisfying conditions impermeability on the surface body from the free vortices left and right wing; L is the number of control points (collocation points), equal to the number of attached vortices on the right wing console.

In the linear formulation, for small angle of attack of the wing-body combination ($\alpha \ll 1$) and small wing tilt angle (angle of inclination wing) ($\delta \ll 1$) solution can be writing as a linear function of the angle of attack and wing tilt angle

$$\Gamma_i = \Gamma_i^\alpha \cdot \alpha + \Gamma_i^\delta \cdot \delta \quad (2)$$

wherein right parts system of algebraic linear equations (1) can be represented as

$$\mathbf{F}_j = \mathbf{F}_j^\alpha \cdot \alpha + \mathbf{F}_j^\delta \cdot \delta \quad (3)$$

where $\Gamma_i^\alpha, \Gamma_i^\delta, \mathbf{F}_j^\alpha, \mathbf{F}_j^\delta$ are derivatives of the $\Gamma_i, \Gamma_i, \mathbf{F}_j, \mathbf{F}_j$ on the angle of attack α and wing tilt angle δ .

To solve the problem the wing-body interference with the fuselage of an arbitrary cross-section for calculating the right parts of the system (1) is proposed to use the panel method that leads to the solution of algebraic linear equations (4)

$$[A][\sigma] = [R] \quad (4)$$

where σ is a column vector

$$\sigma = \sigma^\alpha \alpha + \sigma^\delta \delta \quad (5)$$

Let's give the final formula for the components of the induced velocity for example for case of circular cross-section of the fuselage in j -th control point of the wing panel

$$V_{nj} = V_{zj} \cos \delta = \cos \delta \left\{ V_\infty \sin \alpha_B \left[1 + \frac{R^2 (y_j^2 - z_j^2)}{(y_j^2 + z_j^2)^2} \right] - \frac{\Gamma_i}{2\pi} \left[\frac{y_j - \tilde{y}_v}{(y_j - \tilde{y}_v)^2 + (z_j - \tilde{z}_v)^2} - \frac{y_j + \tilde{y}_v}{(y_j + \tilde{y}_v)^2 + (z_j - \tilde{z}_v)^2} \right] \right\} \quad (6)$$

where V_{nj} is a normal velocity component to the surface at the j -th control point wing panel; induced velocity component along the OZ -axis of the cylinder in crossflow; $(y_j, z_j), (\tilde{y}_v, \tilde{z}_v)$ are coordinates of the control point and the inversion vortex point (see Fig. 1), respectively. Coordinates inversion vortices are by Milne-Thomson's theorem about the circle [38]. The intensity Γ_i and the coordinate y_i of the free vortex can be found on the connection equations [37, 39].

Thus, the problem of the wing-fuselage interference is reduced to the solution (1) to the right side (6) or right-hand sides, obtained by solving the linear algebraic equation system (4), which provides a solution of the problem for the potential flow around an arbitrary contour on the basis of the panel method. An agreement of the velocity field on the surface wing and on the surface fuselage is provided by successive iterations, each of which is reduced to the solution of systems linear algebraic equations (1) with corrected right sides (6). The solution of the problem can be got if as the zero-iteration was selected the solution for isolated wing only. The proposed model it allows get solution for the linear formulation for small angles of attack and the angle of the wing installation two problems at once, which will be called: $\alpha\alpha$ -problem (fuselage and wing have the same angle of attack, angle of the wing tilt angle equal zero); $\delta 0$ -problem (the fuselage has a zero angle of attack and the wing has δ tilt angle). In the linear case, the formula for the coefficients of the normal forces of the wing and the body are of the form (7)

$$\begin{aligned} C_{L W(B)} &= C_{L_\alpha W(B)} \alpha + C_{L_\delta W(B)} \delta, \\ C_{L B(W)} &= C_{L_\alpha B(W)} \alpha + C_{L_\delta B(W)} \delta, \\ C_{L_\alpha W,B} &= C_{L_\alpha W(B)} + C_{L_\alpha B(W)}, \quad C_{L_\delta W,B} = C_{L_\delta W(B)} + C_{L_\delta B(W)}. \end{aligned} \quad (7)$$

The values $C_{L_\alpha W(B)}, C_{L_\delta W(B)}$ are obtained from the solution $\alpha\alpha$ -problem, and the values $C_{L_\alpha B(W)}, C_{L_\delta B(W)}$ – from the solution $\delta 0$ -problem.

3 Review of calculation results

Figs. 4-9 are presented comparing the calculation results obtained by the above theoretical model with calculations by the DVM for case $\alpha\alpha$ -problem [33, 35, 36]. The rectangular, triangular, and swept wings were considered. It may be noted is enough good agreement of calculated data.

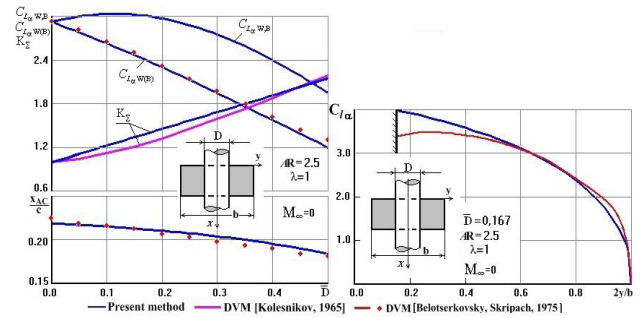


Figure 4. Theoretical results lift-curve slopes vs dimensions diameter of the fuselage (a); Distribution lift-curve slopes along span of the rectangular wing for case midwing-body combination (b)

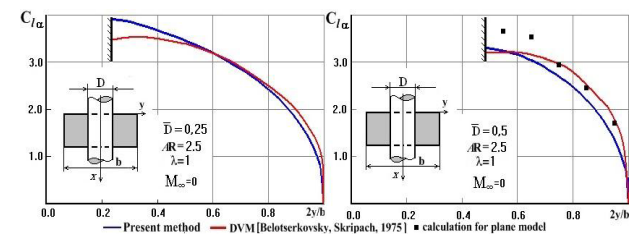


Figure 5. Distribution lift-curve slopes along span of the rectangular wing for case midwing-body combination

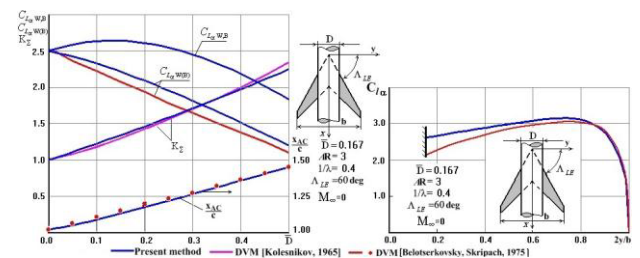


Figure 6. Theoretical results lift-curve slopes vs dimensionless diameter of the fuselage (a); Distribution lift-curve slopes along span of the swept wing for case midwing-body combination (b)

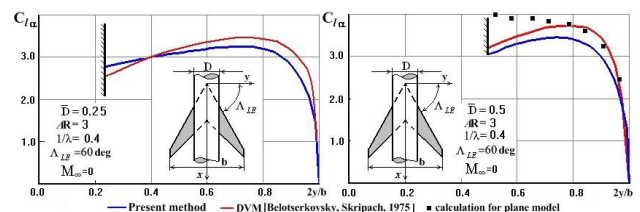


Figure 7. Distribution of the lift-curve slopes along span of the swept wing for case midwing-body combination

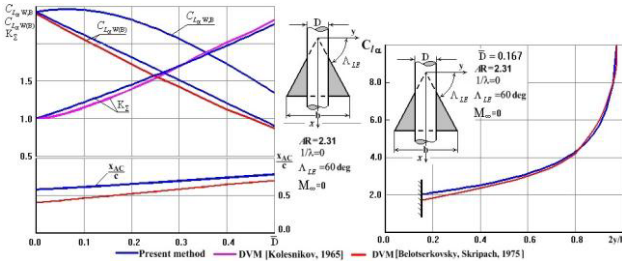


Figure 8. Theoretical results lift-curve slopes vs dimensionless diameter of the fuselage (a); Distribution lift-curve slopes along span of the triangular wing for case midwing-body combination (b)

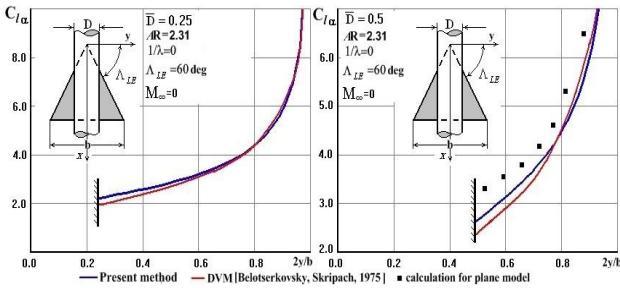


Figure 9. Distribution of the lift-curve slopes along span of the triangular wing for case midwing-body combination

Figs. 4, 6 and 8 also shows the changing in the aerodynamic centre coordinates measured from the beginning of the mean aerodynamic chord. The value K_{Σ} in these figures is defined by the formula

$$K_{\Sigma} = \frac{C_{L\alpha W,B}}{C_{L\alpha W}}, \quad (8)$$

where $C_{L\alpha W}$ is a lift-curve slope for isolated wing for isolated wing, composed of two consoles.

Fig. 10 is presented comparing the calculation results obtained by the above theoretical model with calculations by the numerical method of singularities for case $\delta 0$ -problem [31].

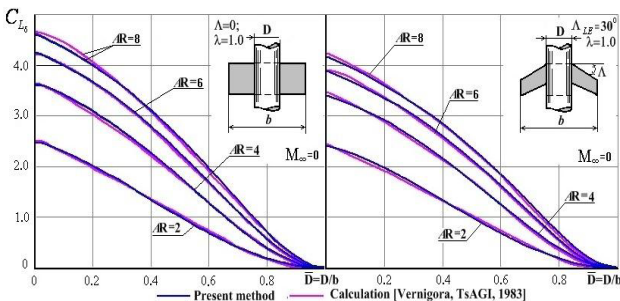


Figure 10. Theoretical results lift-curve slopes vs dimensionless diameter of the fuselage for case $\delta 0$ -problem for case midwing-body combination

Figs. 11-13 shows a comparison of calculated data for the mathematical model described above and the calculated and experimental data of other researchers [40-45].

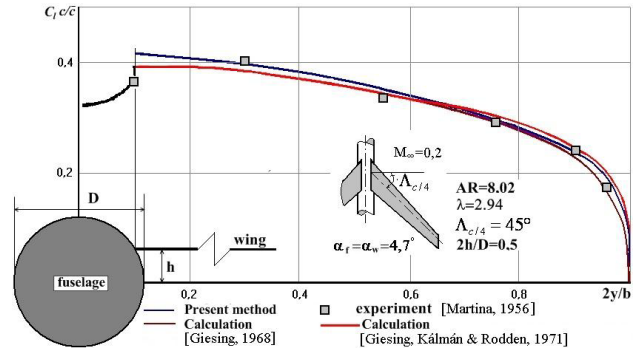


Figure 11. Lift coefficient distribution along span of the sweep wing for case high-wing monoplane

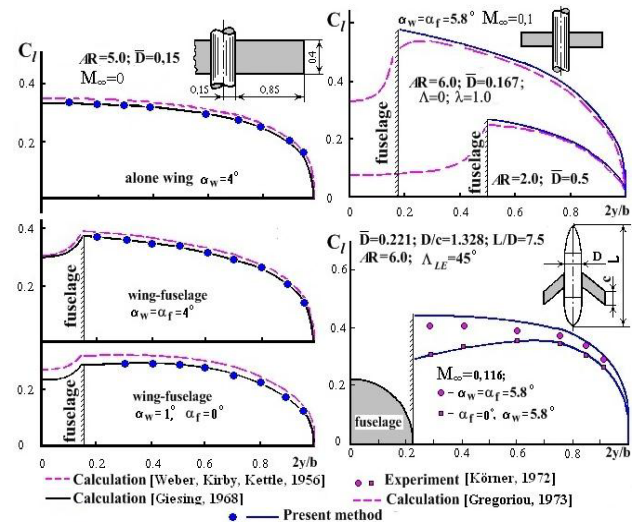


Figure 12. Distribution lift coefficient along span of the midwing-body combination

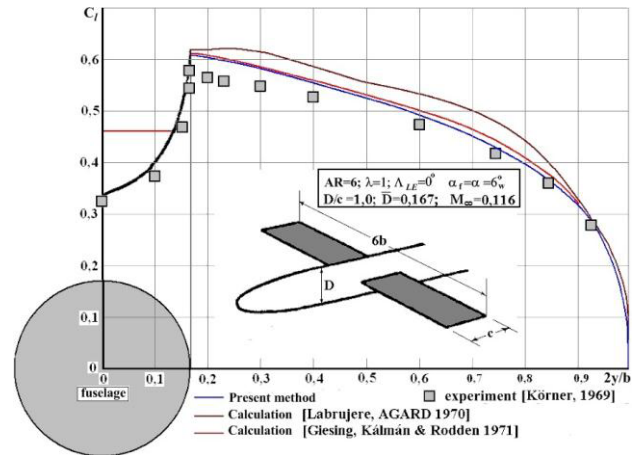


Figure 13. Distribution lift coefficient along span of the rectangular wing for case midwing-body monoplane

An influence of compressibility on values of theoretical lift-curve slopes can see in Figs. 14 and 15. Fig. 14 show results for midwing-body monoplane configuration for rectangular and triangular wings and Fig. 15 show results for high wing-body monoplane configuration for rectangular and triangular wings also [34].

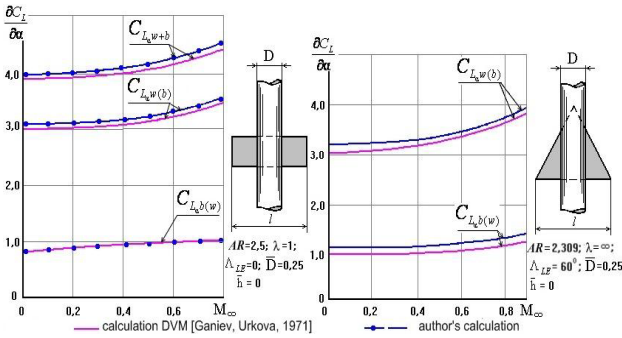


Figure 14. Theoretical results lift-curve slopes vs Mach number

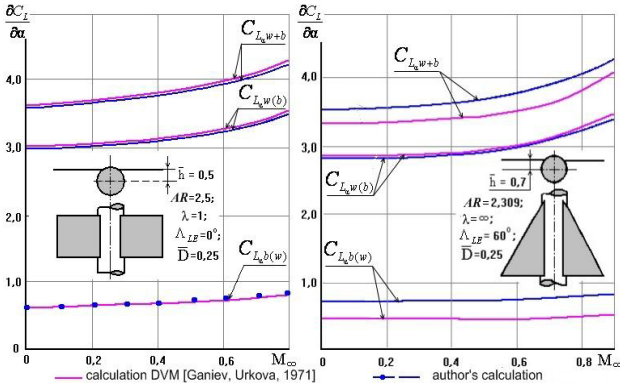


Figure 15. Theoretical results lift-curve slopes vs Mach number

4 Optimization problem for lift-curve slope of for midwing-body monoplane configuration

The review given above it was noted that in a number of theoretical and experimental papers devoted to the wing-body interference, revealed the presence of a maximum in the dependence $\partial C_L / \partial \alpha = f(D/b)$. The carried out calculations on the offered mathematical model also confirms this fact. Generally, the maximum lift-curve slopes for wing-body combination may depend on the cross-sectional shape of the fuselage and shape of the wing. In this paper solutions of the optimization problem for the wing-body combinations with circular and elliptical cross-sections and trapezoidal unswept wings are considered.

The optimization problem is formulated as a nonlinear programming problem as follows:

$$\max C_{L_{\alpha W,B}}(\mathbf{X}), \quad \mathbf{X} \in E^n \quad (9)$$

where $\mathbf{X} = [x_1, x_2, 0]^T$ is a vector of the project parameters connected with geometrical characteristics of the wing-body configuration by formulates

$$\bar{D} = \frac{D}{b} = \frac{1}{x_1^2 + 1}, \quad \frac{1}{\lambda} = \frac{1}{x_2^2 + 1}, \quad (10)$$

where x_1 and x_2 are auxiliary variables. The problem (8), (9) is a problem of unconditional optimization, for which

there are $\bar{D} \in [0;1]$, $(1/\lambda) \in [0;1]$ and $x_1 \in [-\infty; +\infty]$, $x_2 \in [-\infty; +\infty]$.

5 Results of the optimization problem for lift-curve slope for midwing-body monoplane configuration

Figs. 16, 17 show results of the optimization problem for lift-curve slope for midwing-body monoplane configuration with circular cross-section fuselage vs the aspect ratio of the rectangle wing. In Fig. 16 is used the notation

$$\bar{K}_{\Sigma} = \frac{C_{L_{\alpha W,B}}}{C_{L_{\alpha W}}}, \quad (11)$$

where $C_{L_{\alpha W,B}}$ is the lift-curve slope of the wing-body combination same as (8), $\bar{C}_{L_{\alpha W}}$ is a lift-curve slope of the isolated wing in which it is included part of the occupied fuselage.

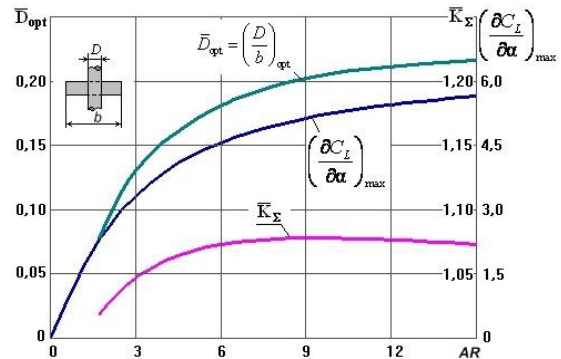


Figure 16. Optimal dimensionless diameter of the mid-wing configuration with circular cross-section body vs the aspect ratio of the rectangular wing

Fig. 17 show results of the optimization problem for lift-curve slopes for midwing-body monoplane configuration with elliptical cross-section fuselage vs the aspect ratio of the rectangular wing. It was revealed that maximums of the lift-curve slopes for the optimal mid-wing configuration with elliptical cross-section body had a sufficiently large relative width of the body (more than 30% of the span wing).

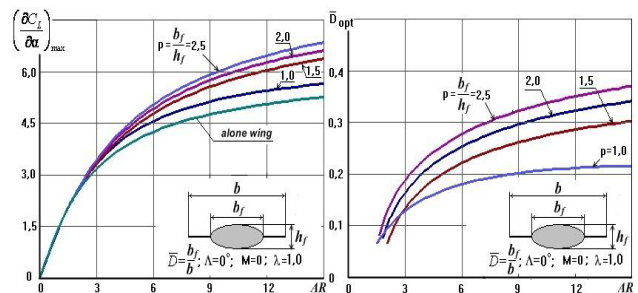


Figure 17. Maximums of the lift-curve slopes for the optimal mid-wing configuration with elliptical cross-section body vs the aspect ratio of the rectangular wing

Fig. 18(a) shows the influence of compressibility on optimal dimensionless diameter vs the aspect ratio of the rectangular wing. Fig. 18(b) also shows statistics for modern aircraft. It is possible to be noted one point (red colour) for the project of fifth-generation aircraft (project M-60, Russia). The project M-60 differs from all other aircraft by the presence of wide fuselage. One can predict that with increasing wing aspect ratio to a value equal 15, the optimal ratio of the width of the fuselage to the wing span can reach approximately 20%.

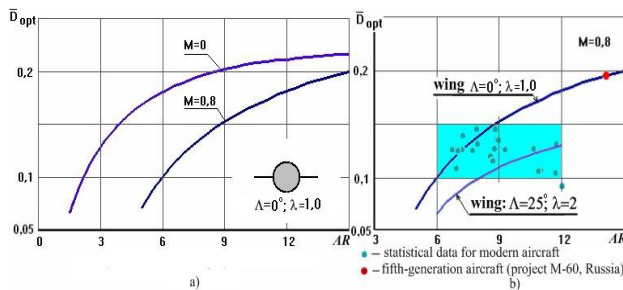


Figure 18. Effect compressibility on dimensionless optimal diameter of the fuselage for case rectangular midwing-body combination

6. Conclusions

The paper gave a brief overview of the works on the wing-body interference. The theoretical approximate model for calculating of the lift-curve slope for wing-body configuration with elliptical cross-section fuselage was considered. The optimization solution of the problem was presented. The present results of the optimization problem for the wing-body combination allowed to select the optimal geometric characteristics for configuration to maximize the values of the lift-curve slopes of the wing-body combination. It was revealed that maximums of the lift-curve slopes for the optimal mid-wing configuration with elliptical cross-section body had a sufficiently large relative width of the body (more than 30% of the span wing).

References

1. E.N. Jacobs, K.E. Ward, NACA Report, **540**, (1935)
2. W.C. Pitts, J.N. Nielsen, G.E. Kaattari, NACA Report, **1307**, (1957)
3. W. Schneider, AGARD CP, **35**, (1968)
4. D.A. Kirby, A.G. Hepworth, R&M, **3747**, (1971)
5. H. Körner, ZFF, **20**, (1972)
6. S.F. Korner, *Fluid-Dynamic Lift* (1985)
7. A.I. Golubinsky, Proceedings TsAGI, **810**, (1961)
8. B.F. Lebedev, Proceedings TsAGI, **719**, (1958)
9. A.A. Dorodnitsyn, Proceedings TsAGI, **546**, (1944)
10. V.V. Keldysh, Proceedings TsAGI, **759**, (1959)
11. V.V. Keldysh, Scientists Notes TsAGI, **VI**, 5, (1975)

12. V.V. Keldysh, Scientists Notes TsAGI, **VIII**, 3, (1977)
13. A.H. Flax, J. Aircraft, **11**, 5, (1974)
14. A.H. Flax, J. Aeron. Sc., **20**, 7, (1953)
15. A.H. Flax, H.R. Lawrence, *Third Anglo-American Aeron. Conf.* (Brighton, 1951)
16. H.R. Lawrence, A.H. Flax, J. Aeron. Sc., **21**, 5, (1954)
17. J.N. Nielsen, *Missile aerodynamics* (McGraw-Hill Book Company, Inc., New York-Toronto-London, (1960)
18. J.R. Spreiter, NACA TN, **1662**, (1948)
19. J.R. Spreiter, NACA TN, **1897**, (1949)
20. J.R. Spreiter, NACA Report, **962**, (1950)
21. J.R. Spreiter, A.H. Sacks, NACA Report, **1296**, (1956)
22. C. Ferrari, *Aerodynamic components of aircraft at high speeds, Vol. VII. High Speed Aerodynamics and Jet Propulsion* (Princeton University Press, Princeton, New Jersey, 1959)
23. E. Karafoli, *Aerodynamics of Aircraft Wing*, AN USSR Publishing, (1956)
24. U.A. Ruhgov, Proceedings TsAGI, **759**, (1959)
25. J. Lennertz, NACA TM, **400**, (1927)
26. J. Lennertz, In: *Durand W. F. (editor) Aerodynamics. Vol. IV*, Springer, Berlin, (1934)
27. A.A. Nikolsky, Proceedings TsAGI, **2122**, (1981)
28. J. Weber, ARC CP, **1331**, (1975)
29. J. Weber, ARC CP, **1332**, (1975)
30. J. Weber, M.G. Joyce, ARC CP, **1334**, (1975)
31. V.N. Vernigora, Proceedings TsAGI, **2176**, (1983)
32. V.I. Kholyavka, *Interference of aircraft parts* Kharkov. Aviation. Inst., Kharkov, (1967)
33. S.M. Belotserkovsky, B. K. Skripach, *Aerodynamic derivatives wing and the aircraft at subsonic speeds*, Nauka, Moscow, (1975)
34. F.I. Ganiev, M. E. Urkova, Proceedings Air Force Academy named after Zhukovsky, **1302**, (1971)
35. G.A. Kolesnikov, Proceedings TsAGI, **810**, (1961)
36. G.A. Kolesnikov, Proceedings TsAGI, **954**, (1965)
37. V.A. Frolov, *Methods for Calculating Lift for Wing-Body Combination*, LAP Lambert Academic Publishing, Saarbrücken, (2011)
38. L.M. Milne-Thomson, *Theoretical Aerodynamics* Constable and Company, London, (1958)
39. M.R. Mendenhall, J. N. Nielsen, NASA CR, **2473**, (1975)
40. J.P. Giesing, McDonnell-Douglas Rep. Douglas Aircraft Co., Report DAC, Vol. I, **67212**, (1968)
41. J.P. Giesing, W.P. Kalman, W.P. Rodden, USAF FDL-TR-71-5, Part I and Part II, (1971)
42. A.P. Martina, NACA TN, **3730**, (1956)
43. H. Körner, Zeitschrift für Flugwissenschaften, **20**, (1972)
44. G. Gregoriou, BMVg-FBWT-73-33, (1973)
45. T.E. Labrujere, W. Loeve, J.W. Slooff, AGARD-CP-71, (1971)